Smart Structures and Systems, *Vol. 33, No. 3 (2024) 217-225*
https://doi.org/10.12989/sss.2024.33.3.217

Compact electromagnetic vibration suppressor and energy harvester; an experimental study

Aref Afsharfard*[1,3], Hooman Zoka [2] and Kyung Chun Kim**[3]

[1] *Department of Mechanical Engineering, Ferdowsi University of Mashhad, Mashhad, Iran*
[2] *Department of Mechanical Engineering, Concordia University, Montreal, Canada*
[3] *Eco-friendly Smart Ship Parts Technology Innovation Center, Pusan National University, Busan, South Korea*

(*Received October 19, 2021, Revised March 31, 2023, Accepted January 28, 2024*)

Abstract. In this study, an electromagnetic dynamic vibration suppressor and energy harvester is designed and studied. In this system, a gear mechanism is used to convert the linear motion to continuous rotary motion. Governing equations of motion for the system are derived and validated using the experimental results. Effects of changing the main parameters of the presented system, such as mass ratio, stiffness ratio and gear ratio on the electro-mechanical behavior of system are investigated. Moreover, using so-called Weighted Cost Function, the optimum parameters of the system are obtained. Finally, it is shown that the presented electromagnetic dynamic vibration absorber not only can reduce the undesired vibration of the main system but also it can harvest acceptable electrical energy.

Keywords: dynamic vibration absorber; electromagnetic energy harvesting; gear mechanism

1. Introduction

Dynamic vibration absorbers are combinations of masses, springs, and dampers which are attached to the main vibratory system, to suppress undesired vibrations. This concept is one of the first strategies to attenuate vibrations of the mechanical systems (Frahm 1911). Widespread use of these systems is due to well-established design approaches seeking to find the best properties of them (Marian and Giaralis 2017). Energy harvesting from the vibratory systems is an interesting subject, which is studied by many researchers. Three different methods are mostly used to convert non-useful vibratory energy into useful electrical energy are electrostatic (Wang and Hansen 2014, Zhang *et al*. 2016b), piezoelectric (Adhikari *et al*. 2016, Karimi *et al*. 2016, Madinei *et al*. 2016, Amini *et al*. 2017, Zoka and Afsharfard 2019) and electromagnetic-based methods. Through these methods, electromagnetic is popular for the capacity of producing high power electrical energy (Donelan *et al*. 2008, Halim *et al*. 2015). The electromagnetic method is used in the suspension system of the vehicles (Zhongjie *et al*. 2013, Zhang *et al*. 2017), bridge (Shen *et al*. 2016, Wang *et al*. 2018) or other large-scale structures.

Williams and Yates (Williams and Yates 1996) presented an idea to convert mechanical energy into electrical energy. They used a magnetic vibratory mass inside a coil and produced 0.1 mW electrical power. Tang and Zuo (2012) replace energy dissipating parts of the tuned mass dampers with an electromagnetic energy harvester of a building. They used a three-story building prototype with a tuned mass damper that equipped with a rack and pinion mechanism and DC generator. They utilized different control system and showed that self-powered active and regenerative semi-active controls can reduce vibration of the main system better than the passive one. Hendijanizadeh *et al*. (2013) studied the effectiveness and output power of both rotational and linear electromagnetic harvesters with limited motion. It is demonstrated that the rotational energy harvesters have a better ability than linear systems. Moreover, it is proved that for a specific situation, the amount of power delivered by a rotational electromagnetic harvester can be twice of a linear system. Pirisi *et al*. (2013) presented a system for harvest electric energy from traffic by the permanent-magnet brushless linear generator. The hybrid evolutionary algorithm is utilized to optimize the general effectiveness of the system. To harvest electrical energy from vehicles pass, a speed bump energy harvester is designed and tested by Wang *et al*. (2016). They showed that the harvester including mechanical motion rectifier mechanism can harvest energy three to four times more than the harvester without this mechanism. The portable energy harvester, which is introduced by Zhang *et al*. (2016a) can exchange the railroad track vibrations into electrical energy. In their study, the produced energy is saved in the supercapacitors to use in safety devices or the rail-side equipment. Gonzalez-Buelga *et al*. (2015) introduced an electromagnetic vibration absorber including a damper with an electromagnetic transducer, which works while the electrical resistance is connected to the terminals of the device. The results showed the maximum

*Corresponding author, Ph.D., Associate Professor,
E-mail: afsharfard@um.ac.ir
**Co-corresponding author, Ph.D., Professor,
E-mail: kckim@pusan.ac.kr

ISSN: 1738-1584 (Print), 1738-1991 (Online)

displacement of the main structure can be reduced up to 20% in comparison with a passive device. Salvi and Giaralis (Salvi and Giaralis 2016) presented a dynamic vibration absorber, which tuned for low-frequency structures. This system contains classical linear tuned mass damper, which is connected to an electromagnetic energy harvester. The results showed that damping of the main structure has a great effect on the harvested energy. Shen *et al*. (2016) suggested a pendulum-type electromagnetic system to harvest electrical energy from structures under earthquake excitations. They validated their model with a single-story steel frame model under scaled El-Centro earthquake. Takeya *et al*. (2016) suggested a tuned mass generator consist of the tuned dual-mass system with a linear electromagnetic transducer as a damper. They showed that the tuned mass generator needs to have a strong design against uncertain bridge vibration. Afsharfard (2018) suggested a magnetic impact damper with a permanent magnet impact mass that moves inside a coil. It is shown using this system, more than 33% of undesired kinetic energy can harvest as electrical energy.

In this study, application of an electromechanical system for suppressing vibrations and harvesting electrical energy is studied. To do so, an electromagnetic energy harvester is designed and coupled with the dynamic vibration absorbers. In several previous studies, applications of the electromagnetic-based systems for harvesting energy and suppressing vibrations are studied (Tang and Zuo 2012, Zhongjie *et al*. 2013, Shen *et al*. 2016). Unlike these investigations, in the present study, a gear mechanism is used to convert the oscillatory motion of the dynamic vibration absorber to the uniform rotary motion. To have a constant speed, flywheels can be connected to the shaft of the generator. Consequently, durability and reliability of the DC generator can improve. Furthermore, several mechanisms to transform the bidirectional linear vibration into regulated unidirectional rotational motion are presented in the study of Lin *et al*. (2018). They introduced a new single-shaft mechanism to improve the energy harvester efficiency. Unlike all of the presented systems, a compact three shafts system with one rack, five meshing gears and six mounted bearings are presented in this study. The advantages of the presented system in comparison with other previous studies are as follows:

- Both energy harvesting and vibration suppressing abilities are summarized in the presented system.
- A compact gear mechanism is coupled with a DC generator to make a reliable system, with acceptable energy harvesting.
- To improve the electromechanical model of the DC generator, the inductance of motor is considered.

Notice that, using five meshing gears in the present system increases gear clearance and manufacturing difficulties. It can be one of the main disadvantages of the presented system.

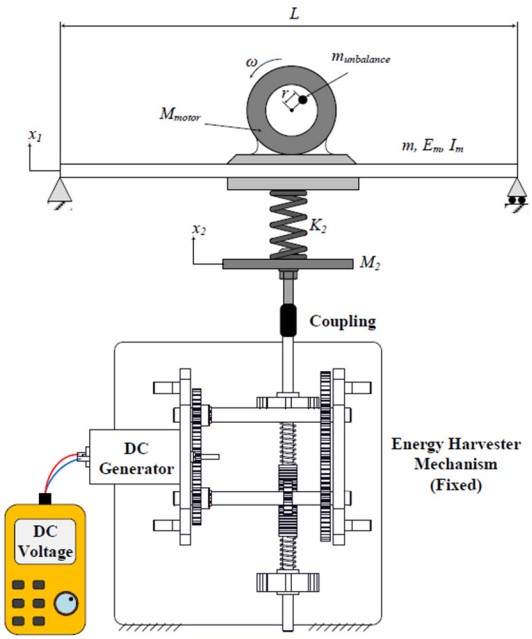

Fig. 1 Schematic of main vibratory system with the electromagnetic dynamic vibration absorber

2. Mathematical model

Consider an eccentric rotating mass, which is connected to the middle of a simply supported beam. Using the classical dynamic vibration absorbers, consist of a linear spring and a mass, which coupled to the energy harvesting system, forced vibration of the beam is attenuated. Schematic of the discussed system is shown in Fig. 1. In this figure, M_{motor}, $m_{\text{unbalance}}$, and m are respectively the mass of the DC motor, the eccentric rotating mass and the mass of the simply supported beam. Also, L and r are the length of the main beam and radius of the rotating mass, respectively. Furthermore, x_1 and x_2 represent the displacement of the main mass and absorber mass. Moreover, M_2 and K_2 are equivalent mass and stiffness of the dynamic vibration absorber. Also, E_{m} and I_{m} are Young's modulus and area moment of inertia of the simply supported beam.

Detailed view of the electromagnetic energy harvester system is shown in Fig. 2. This system included a rack and pinion mechanism, which coupled with dynamic vibration absorber. It can convert the transitional movement of the dynamic vibration absorber to the rotational motion. In Fig. 2 parameters Z_1, Z_2, Z_p and Z_m and R_1, R_2, R_p and R_m are respectively number of gear's teeth and pitch radius of the parts 1, 2, pinion and motor gear. Furthermore, J_1, J_2 and J_{m} and θ_1, θ_2 and θ_{m} are the mass moments of inertia and angle of rotation of the parts 1, 2 and motor shaft, correspondingly. Also, K_3 is equivalent spring stiffness of two same parallel springs, which helps the rack to move back. The relations between the angle of rotation of the shafts and downward and upward motions of the rack can be obtained as follows

$$\begin{cases} \theta_P = \theta_1 = \dfrac{+x_2}{R_P}, \theta_2 = -\theta_1, \theta_M R_M = -\theta_2 R_2; \text{Downward} \\ \theta_P = \theta_1 = -\dfrac{x_2}{R_P}, \theta_M R_M = -\theta_1 R_2; \text{Upward} \end{cases} \quad (1)$$

In this system, two one-way bearings, which are mounted between first and second shafts and gear 2, leads to have unidirectional rotation in the DC generator shaft. Continues and more smooth unidirectional rotation are advantages of using one-way bearings in this system, which cause to harvest more electrical energy.

Equations of motion for downward movement of the system are shown as follows

$$M_1\ddot{x}_1 + (C_1 + C_2)\dot{x}_1 - C_2\dot{x}_2 + (K_1 + K_2)x_1 - K_2x_2 = f \quad (2)$$

$$\begin{matrix} M_2\ddot{x}_2 - C_2\dot{x}_1 + (C_2 + C_3)\dot{x}_2 \\ -K_2x_1 + (K_2 + K_3)x_2 = -f_p \end{matrix} \quad (1)$$

where f and f_p are excitation force and engaged force between rack and pinion. It should be noted that f_p is the reaction force that the fixed electromagnetic energy harvester applies to the vibration absorber. M_1 and K_1 are equivalent mass and spring stiffness of the main system. Furthermore, M_2 and K_2 are mass and spring, which can be shown in Figure 1. C_1 and C_2 are inherent damping of the simply supported beam and the dynamic vibration absorber. Furthermore, C_3 is the equivalent damping of the energy harvester system, which appears because of the bearings and gears of the system. Assuming a harmonic excitation load $f = Fe^{i\omega t}$ leads to deal with harmonic reaction force from electromagnetic energy harvester ($f_p = F_p e^{i\omega t}$) and the receptances can be written as follows

$$\frac{X_1}{F} = \frac{D_{(\omega)} - B_{(\omega)}(F_p/F)}{B_{(\omega)}C_{(\omega)} + D_{(\omega)}A_{(\omega)}} \quad (4)$$

$$\frac{X_2}{F} = \frac{A_{(\omega)}D_{(\omega)} - A_{(\omega)}B_{(\omega)}(F_p/F)}{B^2_{(\omega)}C_{(\omega)} + B_{(\omega)}D_{(\omega)}A_{(\omega)}} \quad 5)$$

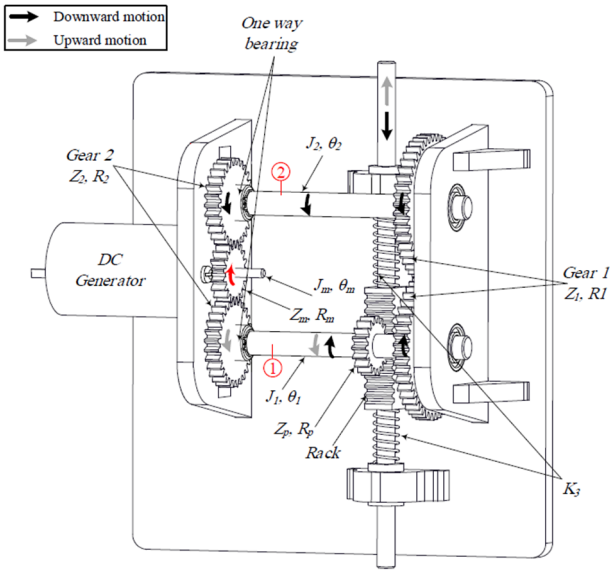

Fig. 2 Detailed view of rectifier of energy harvester

where

$$A_{(\omega)} = M_1\omega^2 + (C_1 + C_2)\omega + K_1 + K_2$$
$$B_{(\omega)} = C_2\omega + K_2$$
$$C_{(\omega)} = -C_2\omega - K_2$$
$$D_{(\omega)} = M_2\omega^2 + (C_2 + C_3)\omega + K_2 + K_3$$

Equations of motion for the gear mechanism, which are coupled with the DC generator, are shown as follows

$$J_1\ddot{\theta}_1 + C_{t_1}\dot{\theta}_1 + K_{t_1}\theta_1 = F_pR_p - F_1R_1 \quad (6)$$

$$J_2\ddot{\theta}_2 + C_{t_2}\dot{\theta}_2 + K_{t_2}\theta_2 = F_1R_1 - F_mR_2 \quad (7)$$

$$J_M\ddot{\theta}_M + C_M\dot{\theta}_M + K_M\theta_M = F_mR_m - k_bI \quad (8)$$

$$L_a\dot{I} + R_aI = k_b\dot{\theta}_m \quad (9)$$

where F_1 and F_m are respectively engaged force between gears 1 and engaged force between gears 2 and gear connected to the shaft of the DC generator. K_{t1}, K_{t2} and K_m and C_{t1}, C_{t2} and C_M are rotational stiffness and rotational damping of shafts 1, 2 and the shaft of DC generator. Moreover, k_b, R_a and L_a are back electromotive force (emf) constant, load resistance and inductance of the electromagnetic transducer (DC generator), and I is the output current of the harvester system. To express the upward motion of the system, Eqs. (2), (3), (8) and (9) can be used. The equation of motion for shafts 1 and 2 can be expressed as follows

$$J_1\ddot{\theta}_1 + C_{t_1}\dot{\theta}_1 + K_{t_1}\theta_1 = F_pR_p - F_1R_1 - F_mR_2 \quad (10)$$

$$J_2\ddot{\theta}_2 + C_{t_2}\dot{\theta}_2 + K_{t_2}\theta_2 = F_1R_1 \quad (11)$$

In this study, a brushed DC motor is used as the electromagnetic transducer because of its high energy density (Tang and Zuo 2012). Unlike previous studies, in this paper, the inductance of the DC motor is considered (Cammarano *et al.* 2010). Note that the mass moment of inertia of the Acrylic made gears are tiny and neglected in this study. Furthermore, in the presented system there is not the rotational spring and rotational resistances in the bearings are considered negligible. The equation of motion for downward and upward movements of the system can be given by

$$M_1\ddot{x}_1 + (C_1 + C_2)\dot{x}_1 - C_2\dot{x}_2 + (K_1 + K_2)x_1 - K_2x_2 = F \quad (12)$$

$$M_2\ddot{x}_2 - C_2\dot{x}_1 + (C_2 + C_3)\dot{x}_2 - K_2x_1 + (K_2 + K_3)x_2 = -(k_bR_2/R_mR_p)I \quad (13)$$

$$L_a\dot{I} + R_aI = (k_bR_2/R_mR_p)\dot{x}_2 \quad (14)$$

Coefficients, which are presented in the above equations, are given in the following relations

$$K_1 = 48E_mI_m/L^3 \quad (15)$$

$$M_1 = M_{\text{motor}} + 0.5m + M_{\text{accelerometer}} \quad (16)$$

$$K_2 = (G_2d_2^4)/(8N_2D_2^3) \quad (17)$$

$$M_2 = 0.4075 + M_{\text{accelerometer}} + M_{\text{coupling}} + M_{\text{shaft}} + M_{\text{spring}}/3 \quad (18)$$

$$K_3 = 2 \times (G_3d_3^4)/(8N_3D_3^3) \quad (19)$$

$$F = 2m_{\text{unbalance}}r\omega^2\sin(\omega t) \quad (20)$$

where $M_{\text{accelerometer}}$, M_{coupling}, M_{shaft}, and M_{spring} are masses of the accelerometer, mechanical coupling, rack shaft and dynamic vibration absorber spring, respectively. In Eq. (18) it should be noted that 0.475 kg is related to the lumped mass of the dynamic vibration absorber, which is connected to the spring K_2. Furthermore, G, N, d and D are the modulus of rigidity, spring turns, diameter of the wire and average diameter of the spring of the dynamic vibration absorber and energy harvester system, respectively. Presented system consists of several mechanical parts and its damping should experimentally be obtained. Note that all damping forces like damping of the vibration absorber, gear box, and other parts will be considered in the experimental measurement. To do so, regarding to the frequency responses shown in part (B) of Fig. 3, and using the peak-picking method, the damping ratios for the first and second natural frequencies ω_1 = 113 rad/s and ω_2 = 208 rad/s are measured as ζ_1 = 0.0052 and ζ_2 = 0.0151. In this study the Rayleigh damping model is used to find the damping matrix. To do so, it is considered the damping is proportional to a combination of the mass and the stiffness matrices as follows

$$\mathbf{c} = \alpha\begin{bmatrix} M_1 & 0 \\ 0 & M_2 \end{bmatrix} + \beta\begin{bmatrix} K_1 + K_2 & -K_2 \\ -K_2 & K_2 + K_3 \end{bmatrix} \quad (21)$$

To find α and β the following relation can be used (Clough and Penzien 2003)

$$\begin{Bmatrix} \alpha \\ \beta \end{Bmatrix} = 2\frac{\omega_1\omega_2}{\omega_2^2 + \omega_1^2}\begin{bmatrix} \omega_2 & -\omega_1 \\ -1/\omega_2 & 1/\omega_1 \end{bmatrix}\begin{Bmatrix} \zeta_1 \\ \zeta_2 \end{Bmatrix} \quad (22)$$

Using the above equation, it can be concluded that α = -0.6247 rad/s and β = 4.5515×10^{-5} s/rad, and the damping matrix can be obtained. Values of the damping coefficients are presented in Table 1.

3. Experimental validation

3.1 Experimental modal testing

The experimental modal analysis is done on the vibratory system, which is shown in part (A) of Fig. 3. To do so, the system is excited by a modal hammer (Global Test AU-02) and the response is captured by accelerometers (Global Test AP2037-100). The signal acquisition is done using National Instruments hardware (NI 9230) with a sample rate of 12.80 kS/s/ch. Note that the sampling rate is higher than necessary to ensure any higher harmonic content is considered (frequency range of interest ≤ 200 Hz). Furthermore, this system represents signals within the passband, as quantified primarily by passband ripple and phase nonlinearity. Each of the measurement is obtained as the spectrum averaging of the responses of ten different impacts, ensuring coherence as much as possible close to the unity. The frequency response of the system is shown in part (B) of Fig. 3. According to this figure, fundamental

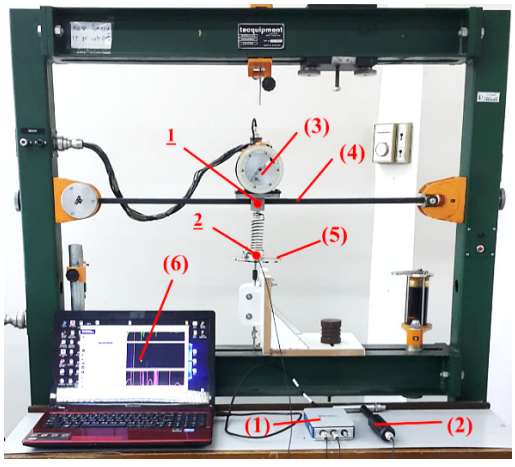

(1) Data acquisition system
(2) Modal Hammer
(3) DC Motor
(4) Main vibratory system
(5) Vibration absorber
(6) Analyzer

(A)

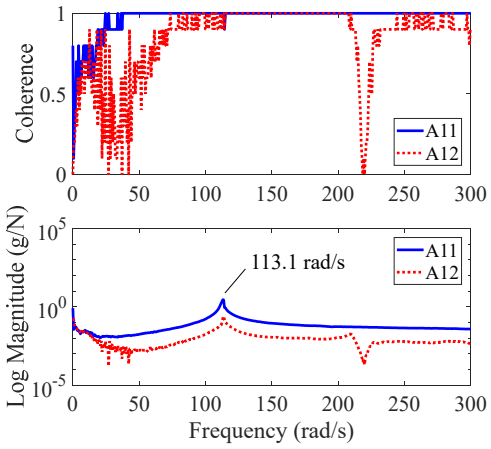

(B)

Fig. 3 Modal test setup (points 1 and 2 are used in modal testing) (A); and frequency response (B)

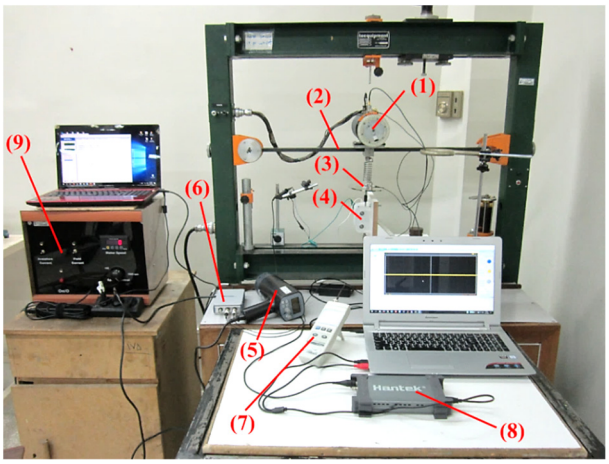

(1) DC motor
(2) Main vibratory system
(3) Dynamic vibration absorber
(4) Energy harvesting system
(5) Stroboscope
(6) Data acquisition system
(7) Portable vibrometer
(8) Oscilloscope

(a)

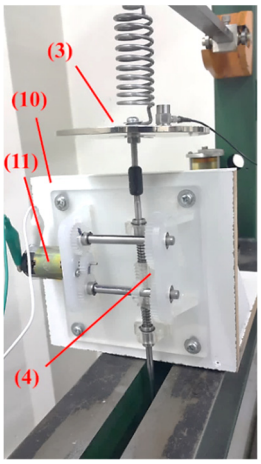

(9) Speed controller
(10) The holder of the system
(11) Electromagnetic transducer

(b)

Fig. 4 Experimental test setup (a) and detailed view of the dynamic vibration absorber attached to the energy harvesting system (b)

frequency of the system is equal to 113.1 rad/s, which is in the frequency range of the exciting system. The second frequency does not appear in modal testing because damping is high in energy harvesting mechanism.

3.2 Electromechanical behavior of the vibratory system

In this section, the electromechanical equation of motion, which is derived in the previous section, is experimentally studied. Part (A) of Fig. 4, shows the test setup system, which is utilized to validate the governing equation of motion. The dynamic vibration absorber and energy harvesting mechanism including the electromagnetic transducer are clearly shown in part (B) of Fig. 4.

Properties of the main beam, dynamic vibration absorber and energy harvesting system are listed in Table 1. In the experimental setup, it should be noted that all the properties of the system are considered constant and K_2 and K_3 are calculated to have a dynamic vibration absorber, which is tuned to work at the natural frequency of the main vibratory system.

The main vibratory system (simply supported beam) is excited using a DC motor with an eccentric mass. The Root Mean Square (RMS) acceleration of the main mass and dynamic vibration absorber mass are measured using IEPE accelerometers (Global Test AP2037-100). Note that the added masses due to the sensors are considered in M_1 and M_2. The output electrical voltage is measured using the Hantek 6022BL USB oscilloscope card. The Landtek digital stroboscope is used to measure the angular velocity of the electromagnetic transducer, during the test. The RMS acceleration of the main vibratory system and dynamic vibration absorber system are respectively shown in parts (A) and (B) of Fig. 5. Furthermore, the RMS acceleration of the main vibratory system without the dynamic vibration absorber is displayed in section (A) of this figure. Regarding this figure, the natural frequency of the main vibratory system is equal to ω = 108.6 rad/s. Also, it can be seen that RMS acceleration of the main system can

Table 1 Properties of the main system and electromagnetic dynamic vibration absorber

Parameters	Values	Parameters	Values	Parameters	Values
L_m (mm)	805.50	R_2 (mm)	15	K_3 (KN/m)	2023
t_m (mm)	12.65	R_m (mm)	10.5	C_1 (N.s/m)	9.79
w_m (mm)	25.31	R_p (mm)	10	C_2 (N.s/m)	158.34
M_{motor} (gr)	5.62	Z_1	47	C_3 (N.s/m)	92.42
$m_{unbalance}$ (gr)	14.3	Z_2	28	k_b (V/rad/s)	0.0458
ρ_m (Kg/m^3)	7498	Z_m	19	L_a (mH)	24
E_m (GPa)	190	Z_p	18	R_a (Ω)	9
G (GPa)	79	K_1 (KN/m)	79.29		
R_1 (mm)	24.5	K_2 (KN/m)	3479		

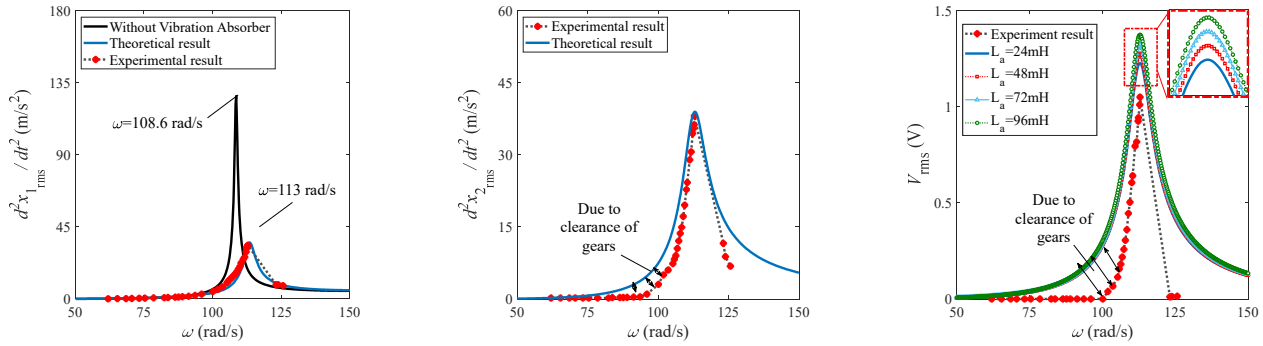

(a) (b) (c)

Fig. 5 Accelerance of the main mass (a); vibration absorber (b); and the RMS output voltage (c)

significantly be reduced by using the dynamic vibration absorber. Agreement between the theoretical and experimental results guarantees accuracy of the presented electro-mechanical equation of motion. The RMS of output electrical voltage versus frequency is shown in part (C) of Fig. 5. Furthermore, in this part, the effect of changing the inductance (L_a) on the output voltage is shown. As shown in this figure, increasing the inductance increases the harvested electrical voltage.

Regarding Fig. 5, it should be noted that during the experimental frequency sweep, an unwanted jump occurs around the natural frequency of the system. Therefore, the measured electrical voltage suddenly decreases. Consequently, the RMS voltage, which is calculated by the USB oscilloscope software, is smaller than the numerical result. Furthermore, several uncertainties in an experimental study, like the gear clearance, leads to a decrease of the generated electrical voltage rather than the numerical result.

In the experimental study, it observed that the gear mechanism during small displacement of the absorber (x_2) is noisy, and the DC generator shaft doesn't rotate. This noise, which is made by contact of gear teeth, is a result of the clearance of the gears. Note that, the impact between gears leads to energy dissipation, and then displacement of the mass of dynamic vibration absorber in the experiment is smaller than the theoretical one. This behavior can be observed in part (B) of Fig. 5. Furthermore, the clearance of the gears explains the no voltage generation during small displacement of the dynamic vibration absorber mass, which is shown in part (C) of Fig. 5. The angular velocity of DC generator is measured 574.5 rpm when excitation frequency is equal to 113 rad/s, but based on the gear ration of the gearbox it should be 128 rad/s. Therefore, the error of the theoretical result is equal to 11.7%. Source of the presented error is unforeseen energy dissipation in the gear mechanism. Note that this energy dissipation occurs during the system application (when the gears are rotating) and the energy dissipation couldn't be covered by the dissipated energy of the damping force, which is measured by the modal test in Fig. 3 (impact hammer excitation).

4. Results and discussion

In this section, the optimized system, which can effectively suppress vibrations and harvest maximum energy, is presented. For this reason, three dimensionless parameters of the system are selected, which simply named as a mass ratio (M_2/M_1), stiffness ratio (K_2/K_1) and gear ratio (Z_m/Z_2). The main aim is to select the best values for these three parameters, which minimize the RMS acceleration of the main vibratory system and maximize the harvested RMS power (P_{rms}). The electro-mechanical behavior of the system is investigated by changing the mass ratio between 0.053 and 0.11 and changing the stiffness ratio between 0.032 and 0.056. Furthermore, five different values (0.31, 0.38, 0.47, 0.57 and 0.68) are considered for gear ratio. In the present study, after making sure about the

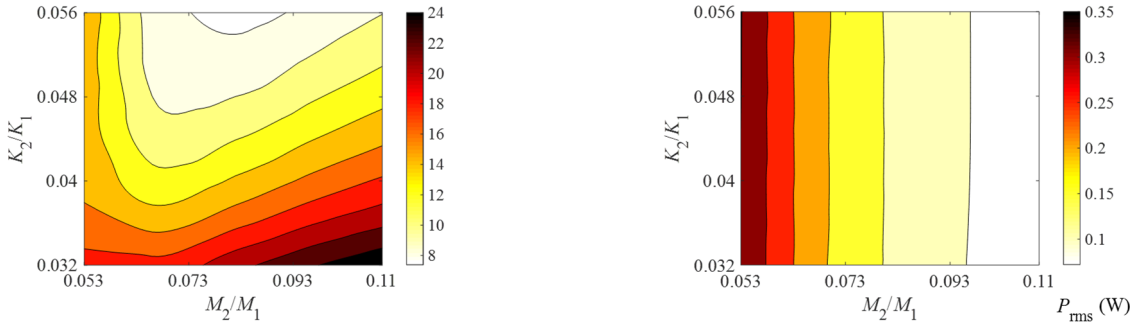

(a) (b)

Fig. 6 Variation of the RMS acceleration of the main beam (a); and RMS output power (b) with changing mass ratio and stiffness ratio ($Z_m/Z_2 = 0.68$)

Table 2 Proper values of the mass ratio and stiffness ratio for different quantities of the gear ratio

Z_m/Z_2	0.31		0.38		0.47		0.57		0.68	
Parameters	M_2/M_1	K_2/K_1	M_2/M_1	K_2/K_1	M_2/M_1	K_2/K_1	M_2/M_1	K_2/K_1	M_2/M_1	K_2/K_1
Vibration-based	0.08	0.056	0.08	0.056	0.07	0.056	0.065	0.056	0.08	0.056
Power-based	0.053	N.E.[1]	0.053	N.E.	0.053	N.E.	0.053	N.E.	0.053	N.E.

[1] No Effect

accuracy of the presented theoretical equations of motion, for the above-mentioned gear ratios, the values of maximum acceleration of the main system and the RMS output power are obtained by changing the mass ratio and stiffness ratio. A curve is fitted to the results using the curve fitting toolbox of MATLAB software. Then according to obtained curves, it is concluded that to decrease the vibration amplitude and increase the harvested power, the mass ratio should be selected between 0.06 and 0.11 and stiffness ratio should be considered between 0.038 and 0.056. At here, it should be noted that the selected mass ratios are 0.052, 0.067, 0.083, 0.097 and 0.111. Furthermore, the stiffness ratios are 0.032, 0.038, 0.044, 0.050 and 0.057. Effects of varying the mass ratio and stiffness ratio on RMS acceleration of the main vibratory system and the harvested power, when the gear ratio is 0.68, are respectively shown in parts (a) and (b) of Fig. 6. The proper values for mass ratio and stiffness ratio in all values of gear ratio are presented in Table 2. In this table, the power-based and energy-based rows respectively refer to the system, which can strongly suppress vibrations and effectively harvest energy.

Table 2 shows that stiffness ratio 0.056 is a proper value for the discussed system. Furthermore, regarding this table, it can be concluded the mass ratio should be selected between 0.053 and 0.08. To design a system, which can effectively maximize harvested energy and minimizing vibrations, the following Weighted Cost Function (WCF) is presented as follows (Afsharfard and Farshidianfar 2014). Note that, this parameter summarizes both of vibration-based and power-based designs in a parameter.

$$WCF\ (\%) = \left\{\left(WF_1 \times \frac{P}{P_{\max}}\right) + \left(WF_2 \times \frac{\ddot{x}_1}{\ddot{x}_{1\max}}\right)\right\} \times 100 \quad (23)$$

where WF_1 and WF_2 are respectively the weight factors for the power-based and vibration-based designs and $P_{\max}$ is the maximum output power. Also, $\ddot{x}_{1max}$ and $\ddot{x}_1$ are maximum RMS acceleration and RMS acceleration of the main vibratory system. The best mass ratio and stiffness ratio to reach maximum WCF values are shown in Table 3. According to this table, maximum WCF value can be obtained while $Z_m/Z_2 = 0.38$. Note that, decreasing the gear ratio usually results in increasing the WCF value.

Considering $WF_1 = 0.5$, best parameters of the system are equal to $Z_m/Z_2 = 0.38$, $K_2/K_1 = 0.056$ and $M_2/M_1 = 0.053$, which leads to harvest 1.2 W electrical power. Time response of the main vibratory system in its fundamental frequency (ω = 108.6 rad/s) with optimized dynamic vibration absorber is shown in part (a) of Fig. 7. In this figure, the vibration amplitude of the main system in its resonance frequency is equal to 1.5 cm, which decreases more than 88.6% with the presented dynamic vibration absorber system. In this situation, the oscillation amplitude of the dynamic vibration absorber, which is transmitting to the gear mechanism, is 2.33 mm. Generated power due to this small oscillation is shown in part (b) of Fig. 7. In this figure, the beating like variations of the maximum or minimum of the harvested power is due to frictional torque

Table 3 Values of M_2/M_1 and K_2/K_1 for different values of Z_m/Z_2 to have a maximum weighted cost function

Z_m/Z_2	K_2/K_1	M_2/M_1	*WCF* (%)		
			$WF_1 = 0.2$	$WF_1 = 0.5$	$WF_1 = 0.8$
0.31	0.056	0.053	90.29	93.70	97.12
0.38	0.056	0.053	90.78	94.24	97.70
0.47	0.056	0.053	89.08	90.15	91.22
0.57	0.056	0.053	86.26	83.79	81.31
0.68	0.056	0.053	82.98	76.53	70.08

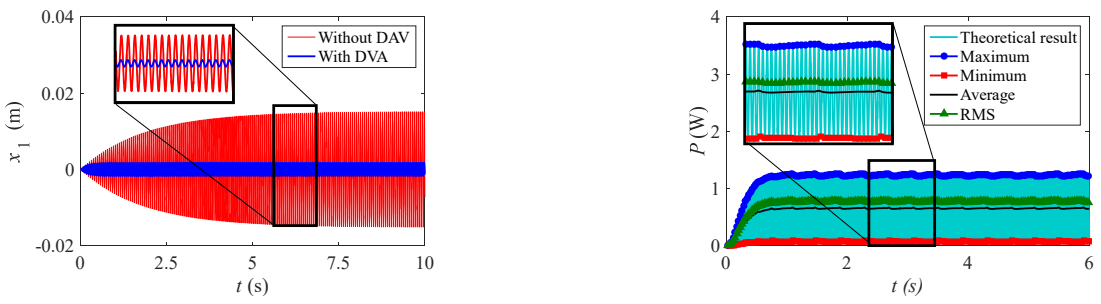

(a) (b)

Fig. 7 Time response of the main system with and without dynamic vibration absorber (A); and time response of the harvested power in (ω = 108.6 rad/s, $WF_1 = 0.5$, $Z_m/Z_2 = 0.38$, $K_2/K_1 = 0.056$ and $M_2/M_1 = 0.053$)

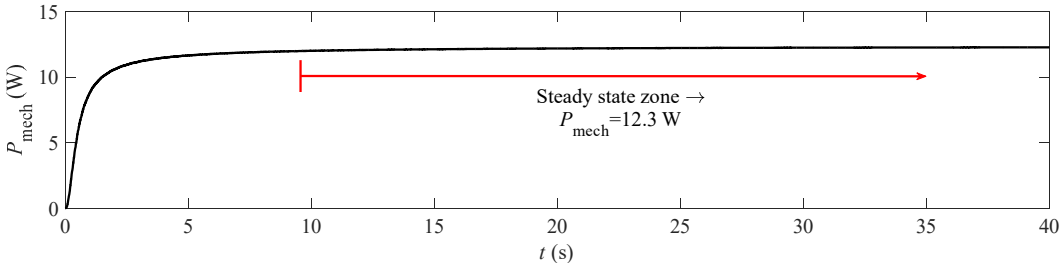

Fig. 8 Mechanical power versus time (ω = 108.6 rad/s, Z_m/Z_2 = 0.38, K_2/K_1 = 0.056 and M_2/M_1 = 0.053)

against the rotation of DC generator armature and little mass moment of inertia of the armature. In Fig. 9, the RMS of harvested power is about 0.77 W and the maximum value of harvested power is about 1.2 W.

To have an approximation about the harvested energy, mechanical power of the dynamic vibration absorber, which is connected to the presented energy harvesting system, is compared with the output electrical voltage. To do so, the following relation is used to calculate the mechanical power

$$P_{\text{mech}} = \left(\sum_{i=1}^{n} \frac{1}{2} M_2 (\dot{x}_2)_i^2 + \frac{1}{2} K_2 (x_2 - x_1)_i^2 \right) / t_n \quad (24)$$

where i is the step number. Fig. 8 shows the mechanical output power versus time in the frequency of ω = 108.6 rad/s. As shown in this figure, the mechanical power, in its steady state, is equal to 12.3 W. Therefore, the energy harvester can convert 9.8% of the mechanical power into electrical power (Efficiency = 9.8%). Note that, improving clearance of the gears in the presented mechanism and using the flywheel and high-efficiency generator can improve the efficiency of the system.

5. Conclusions

In this paper, a compact electromagnetic dynamic vibration absorber is used to decrease undesired vibrations and harvest electrical energy. To do so, three parallel shafts are used to make a small size system, which its generator is located between shafts, and whole of system can easily be embedded in a compact box. Governing electromechanical equations of motion for this system is derived and experimentally validated. It is shown that the introduced system can effectively suppress undesired vibration of the main system. It is shown that the presented system can reduce undesired vibrations of the main system up to 90.5%. Moreover, it is displayed the system can generate electrical power, which can be used by outer consumers or by active control devices. To improve performance of the discussed vibration suppressor and energy harvester, three non-dimensional parameters are considered and using the presented weighted cost function, the optimum values for these parameters are obtained. To do so, the goal function is maximizing the harvested power and minimizing the vibration amplitude of the main system in natural frequency. Results showed that the presented small device can decrease the RMS acceleration of the main vibratory system up to 88.5% and also it can convert 9.8% of the total mechanical power of the dynamic vibration absorber into electrical power.

Acknowledgments

This work was supported by Brain Pool Program through the National Research Foundation of Korea (NRF) funded by Ministry of Science and ICT (RS-2023-00304351).

This work was also supported by the National Research Foundation of Korea (NRF) grant, which is funded by the Korean government (MSIT) (No. 2020R1A5A8018822).

References

Adhikari, S., Friswell, M.I., Litak, G. and Khodaparast, H.H. (2016), "Despign and analysis of vibration energy harvesters based on peak response statistics", *Smart Mater. Struct.*, **25**(6), p. 065009. https://doi.org/10.1088/0964-1726/25/6/065009

Afsharfard, A. (2018), "Application of nonlinear magnetic vibro-impact vibration suppressor and energy harvester", *Mech. Syst. Signal Process.*, **98**(Supplement C), 371-381. https://doi.org/10.1016/j.ymssp.2017.05.010

Afsharfard, A. and Farshidianfar, A. (2014), "Application of single unit impact dampers to harvest energy and suppress vibrations", *J. Intell. Mater. Syst. Struct.*, **25**(14), 1850-1860. https://doi.org/10.1177/1045389X14535012

Amini, Y., Heshmati, M., Fatehi, P. and Habibi, S.E. (2017), "Piezoelectric energy harvesting from vibrations of a beam subjected to multi-moving loads", *Appl. Mathe. Modell.*, **49**, 1-16. https://doi.org/10.1016/j.apm.2017.04.043

Cammarano, A., Burrow, S.G., Barton, D.A.W., Carrella, A. and Clare, L.R. (2010), "Tuning a resonant energy harvester using a generalized electrical load", *Smart Mater. Struct.*, **19**(5), p. 055003. https://doi.org/10.1088/0964-1726/19/5/055003

Clough, R.W. and Penzien, J. (2003), *Dynamics of Structures*, Computers & Structures, New York, USA.

Donelan, J.M., Li, Q., Naing, V., Hoffer, J.A., Weber, D.J. and Kuo, A.D. (2008), "Biomechanical energy harvesting: generating electricity during walking with minimal user effort", *Science*, **319**(5864), p. 807. https://doi.org/10.1126/science.1149860

Frahm, H. (1911), *Device for Damping Vibrations of Bodies*.

Gonzalez-Buelga, A., Clare, L.R., Neild, S.A., Burrow, S.G. and Inman, D.J. (2015), "An electromagnetic vibration absorber with harvesting and tuning capabilities", *Struct. Control Health Monitor.*, **22**(11), 1359-1372. https://doi.org/10.1002/stc.1748

Halim, M.A., Cho, H. and Park, J.Y. (2015), "Design and

experiment of a human-limb driven, frequency up-converted electromagnetic energy harvester", *Energy Convers. Manage.*, **106**, 393-404. https://doi.org/10.1016/j.enconman.2015.09.065

Hendijanizadeh, M., Sharkh, S.M., Elliott, S.J. and Moshrefi-Torbati, M. (2013), "Output power and efficiency of electromagnetic energy harvesting systems with constrained range of motion", *Smart Mater. Struct.*, **22**(12), p. 125009. https://doi.org/10.1088/0964-1726/22/12/125009

Karimi, M., Karimi, A.H., Tikani, R. and Ziaei-Rad, S. (2016), "Experimental and theoretical investigations on piezoelectric-based energy harvesting from bridge vibrations under travelling vehicles", *Int. J. Mech. Sci.*, **119**(Supplement C), 1-11. https://doi.org/10.1016/j.ijmecsci.2016.09.029

Kim, P. and Seok, J. (2015), "Dynamic and energetic characteristics of a tri-stable magnetopiezoelastic energy harvester", *Mech. Mach. Theory*, **94**, 41-63. https://doi.org/10.1016/j.mechmachtheory.2015.08.002

Li, Z., Zuo, L., Kuang, J. and Luhrs, G. (2013), "Energy-harvesting shock absorber with a mechanical motion rectifier", *Smart Mater. Struct.*, **22**(2), p. 025008. 10.1088/0964-1726/22/2/025008

Lin, T., Wang, J.J. and Zuo, L. (2018), "Efficient electromagnetic energy harvester for railroad transportation", *Mechatronics*, **53**, 277-286. https://doi.org/10.1016/j.mechatronics.2018.06.019

Madinei, H., Khodaparast, H.H., Adhikari, S. and Friswell, M.I. (2016), "Design of MEMS piezoelectric harvesters with electrostatically adjustable resonance frequency", *Mech. Syst. Signal Process.*, **81**, 360-374. https://doi.org/10.1016/j.ymssp.2016.03.023

Marian, L. and Giaralis, A. (2017), "The tuned mass-damper-inerter for harmonic vibrations suppression, attached mass reduction, and energy harvesting", *Smart Struct. Syst., Int. J.*, **19**(6), 665-678. https://doi.org/10.12989/sss.2017.19.6.665

Pirisi, A., Mussetta, M., Grimaccia, F. and Zich, R.E. (2013), "Novel speed-bump design and optimization for energy harvesting from traffic", *IEEE Transact. Intell. Transport. Syst.*, **14**(4), 1983-1991. https://doi.org/10.1109/TITS.2013.2272650

Salvi, J. and Giaralis, A. (2016), "Concept study of a novel energy harvesting-enabled tuned mass-damper-inerter (EH-TMDI) device for vibration control of harmonically-excited structures", *J. Phys.: Conference Series*, **744**(1), p. 012082. https://doi.org/10.1088/1742-6596/744/1/012082

Shen, W., Zhu, S. and Zhu, H. (2016), "Experimental study on using electromagnetic devices on bridge stay cables for simultaneous energy harvesting and vibration damping", *Smart Mater. Struct.*, **25**(6), p. 065011. https://doi.org/10.1088/0964-1726/25/6/065011

Takeya, K., Sasaki, E. and Kobayashi, Y. (2016), "Design and parametric study on energy harvesting from bridge vibration using tuned dual-mass damper systems", *J. Sound Vib.*, **361**(Supplement C), 50-65. https://doi.org/10.1016/j.jsv.2015.10.002

Tang, X. and Zuo, L. (2012), "Simultaneous energy harvesting and vibration control of structures with tuned mass dampers", *J. Intell. Mater. Syst. Struct.*, **23**(18), 2117-2127. https://doi.org/10.1177/1045389X12462644

Wang, F. and Hansen, O. (2014), "Electrostatic energy harvesting device with out-of-the-plane gap closing scheme", *Sensors Actuat. A: Phys.*, **211**(Supplement C), 131-137. https://doi.org/10.1016/j.sna.2014.02.027

Wang, J., Lin, T. and Zuo, L. (2013), "High efficiency electromagnetic energy harvester for railroad application", *Proceedings of International Design Engineering Technical Conferences and Computers and Information in Engineering Conference*, Portland, OR, USA, August. https://doi.org/10.1115/DETC2013-12770

Wang, L., Todaria, P., Pandey, A., O'Connor, J., Chernow, B. and Zuo, L. (2016), "An electromagnetic speed bump energy harvester and its interactions with vehicles", *IEEE/ASME Transact. Mechatron.*, **21**(4), 1985-1994. https://doi.org/10.1109/TMECH.2016.2546179

Wang, H., Jasim, A. and Chen, X. (2018), "Energy harvesting technologies in roadway and bridge for different applications – A comprehensive review", *Appl. Energy*, **212**, 1083-1094. https://doi.org/10.1016/j.apenergy.2017.12.125

Williams, C.B. and Yates, R.B. (1996), "Analysis of a micro-electric generator for microsystems", *Sensors Actuat. A: Phys.*, **52**(1), 8-11. https://doi.org/10.1016/0924-4247(96)80118-X

Zhang, X., Zhang, Z., Pan, H., Salman, W., Yuan, Y. and Liu, Y. (2016a), "A portable high-efficiency electromagnetic energy harvesting system using supercapacitors for renewable energy applications in railroads", *Energy Convers. Manage.*, **118**, 287-294. https://doi.org/10.1016/j.enconman.2016.04.012

Zhang, Y., Wang, T., Zhang, A., Peng, Z., Luo, D., Chen, R. and Wang, F. (2016b), "Electrostatic energy harvesting device with dual resonant structure for wideband random vibration sources at low frequency", *Rev. Scientif. Instrum.*, **87**(12), p. 125001. https://doi.org/10.1063/1.4968811

Zhang, Y., Chen, H., Guo, K., Zhang, X. and Li, S.E. (2017), "Electro-hydraulic damper for energy harvesting suspension: Modeling, prototyping and experimental validation", *Appl. Energy*, **199**, 1-12. https://doi.org/10.1016/j.apenergy.2017.04.085

Zhongjie, L., Zuo, L., Kuang, J. and Luhrs, G. (2013), "Energy-harvesting shock absorber with a mechanical motion rectifier", *Smart Mater. Struct.*, **22**(2), p. 025008. https://doi.org/10.1088/0964-1726/22/2/025008

Zhu, S., Shen, W., Zhu, H.P. and Xu, Y.L. (2016), "Electromagnetic energy harvesting from structural vibrations during earthquakes", *Smart Struct. Syst., Int. J.*, **18**, 449-470. https://doi.org/10.12989/sss.2016.18.3.449

Zoka, H. and Afsharfard, A. (2019), "Double stiffness vibration suppressor and energy harvester: an experimental study", *Mech. Syst. Signal Process.*, **121**, 1-13. https://doi.org/10.1016/j.ymssp.2018.11.020